

Design and realisation of leakage channel fibres by the powder-in-tube method

J. Scheuner^a, P. Raisin^a, S. Pilz^b, and V. Romano^{a,b}

^aInstitute of Applied Physics, University of Bern, Sidlerstrasse 5, CH-3012 Bern, Switzerland

^bBern University of Applied Sciences, ALPS, Pestalozzistrasse 20, CH-3400 Burgdorf, Switzerland

ABSTRACT

The applications of fibre lasers demand for increasing power. Limits are set by various nonlinear effects. Leakage channel fibres (LCF) are one approach to this problem. With this type of fibre, most nonlinear effects can, in principle, be mitigated simultaneously by increasing the mode field area and by maintaining the single mode regime. For its implementation, we propose to use the powder-in-tube preform technique. While the microstructure consists of commercial pure silica rods, the surrounding is filled with index-raised aluminum-doped silica oxide granulate. For the fabrication of the latter, we tested two different methods. For the first one, the oxide precursors were mixed in pure powder form. In the other method, the material was produced with the help of the sol-gel process, where the mixing takes place in liquid phase, thus resulting in an expected improved homogeneity. Prior to the fabrication of a prototype, their feasibility has been tested with the help of a finite-difference method simulation tool (Lumerical MODE Solutions). Two such fibres have been fabricated according to this results. The influence of the granulate mixing method and of the grain size on the homogeneity in refractive index has been tested. Although the produced fibres do not yet show the desired performance, the produced prototypes prove that LCFs can indeed be realised with this approach.

Keywords: Leakage channel fibres, large mode area fibres, micro-structured fibres, sol-gel

1. INTRODUCTION

The power scaling of fibre lasers is currently limited by nonlinear effects such as stimulated Raman scattering (SRS), stimulated Brillouin scattering (SBS), self-phase modulation (SPM) and ultimately by optical damage.¹ A quite general approach to avoid or limit these effects is increasing the effective mode area, a procedure which, in effect increases the core diameter.¹ But simply increasing the core diameter in a step index fibre does not solve the problem entirely, especially regarding the fact that single-mode operation is generally desired, in order to avoid beam instability due to mode dispersion. An increase of the core radius reflects itself in an increase of the V-number, which is a measure for the number of modes propagating in a step-index fibre. Per definition, the only possibility to keep it below the single-mode threshold ($V=2.405$) is a decrease of the numerical aperture (and thus the refractive index difference between core and cladding). However, low numerical aperture leads to higher bend losses, which sets an upper limit to the core diameter which is about $20\mu\text{m}$ (assuming core refractive index $n_{\text{core}}=1.45$, wavelength $\lambda=1\mu\text{m}$).²

Large mode area fibres (LMA) follow this straightforward approach.² In addition to the mode field enhancement merely caused by core diameter increase, the fact that higher order modes are more sensitive to bend losses than the fundamental mode, can be exploited.³ Control of launch conditions (i.e. selective mode excitation) allows for single mode propagation over short distances (about 20m) in multimode fibres with core diameters up to $45\mu\text{m}$.⁴

Another category of solutions to the mode area problem, are various forms of micro-structured fibres. Probably the most common form consists of a hexagonally arranged array of air holes running along the fibre,⁵ with a single hole missing in the centre of the fibre section, forming the core. They are commonly termed "holey fibres" or "photonic crystal fibres" (PCF). Core diameters up to $40\mu\text{m}$ have been reported⁶ and are commercially available. Their limitation is, again, given by bend losses. In this model, light is guided in a way which is described in the frame of the so-called "effective index model".⁷ In this way, the guiding essentially occurs via an "average index contrast" between the defect core and the holey structure surrounding it. In fact, with this approach, the

hole-structure does not even have to be periodic.⁸

Up-scaled versions of photonic crystal fibres of several millimetres in diameter have already been developed.⁹ They are generally referred to as "rod-type fibres". These types of fibres have very high core diameters of around $100\mu\text{m}$, their only drawback being their lack of bendability.

Leakage channel fibres arise from the development of holey fibres.¹⁰ The main practical difference in comparison to "conventional" PCFs are the number and size of air holes. Small in number and large in diameter, they provide a large (average) index contrast. The interstices between these holes are the eponym of this type of fibre: Light from the waveguide modes "leaks" through these "channels". Calculations indicate that the effect becomes more pronounced, with rising order of the mode.¹¹ Hence, by a suitable combination of distance between the holes and their diameter, the losses of the fundamental mode can be kept so low, that it propagates over practical distances without significant loss, while the higher order mode losses are so high, that they are practically suppressed. The term "effective single-mode" has been coined to describe this feature.¹² It is worth noting, that the aforementioned "channels" are not really necessary to create leaky modes, as underlined by the example of the W-type planar waveguide.¹³ Most importantly, however, this design theoretically allows for core diameters of around $50\mu\text{m}$ with reasonable bend loss.¹⁰ As a practical improvement, it has been shown that the air holes can be replaced with circular regions of low refractive index (compared e.g. to silica).¹⁴

The most commonly encountered geometrical arrangement in literature consists of six hexagonally arranged air-holes (or low index structural elements) surrounding a central core region (figure 1).^{10,12} Other designs include different variants based on the trigonal lattice,^{12,14–16} circular lattice,¹⁷ as well as polygonal arrangements (e.g. octagonal).¹⁸ Furthermore, alternative shapes for the low-index regions have been proposed. Within this group are hexagons¹⁹ or cylindrical wedges.²⁰

Structured fibres are usually fabricated by means of the stack-and-draw procedure, in which appropriate glass rods and/or capillaries are arranged in correspondence to the aimed structure.²¹ Although it does not seem to be explicitly mentioned in the publications, the same applies for the case of leakage channel fibres. Our approach is based on the powder-in-tube method, in which large parts of the preform consist of a form of granulate.²² The glass transition of the granulate then takes place either beforehand by thermal annealing (vitrification) or directly during fibre drawing. In short, our proposed fabrication procedure is as follows: commercial silica rods with circular cross-section forming the structure are placed inside a silica tube closed at the bottom. The remaining space is then filled with self-made Al-doped granulate with a higher refractive index with respect to silica (figure 2). This preform is then placed in a fibre drawing furnace, evacuated from the top and drawn into a fibre.

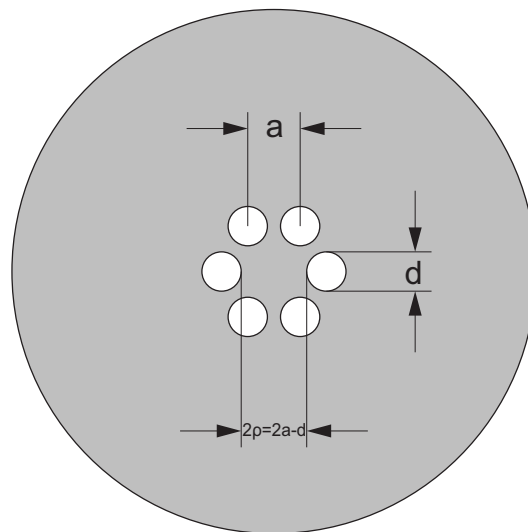


Figure 1. Schematic of the most common leakage channel fibre design. The refractive index of the white circles is smaller than the one of the surrounding grey region. a : pitch, d : hole or structural element diameter, ρ : core radius.

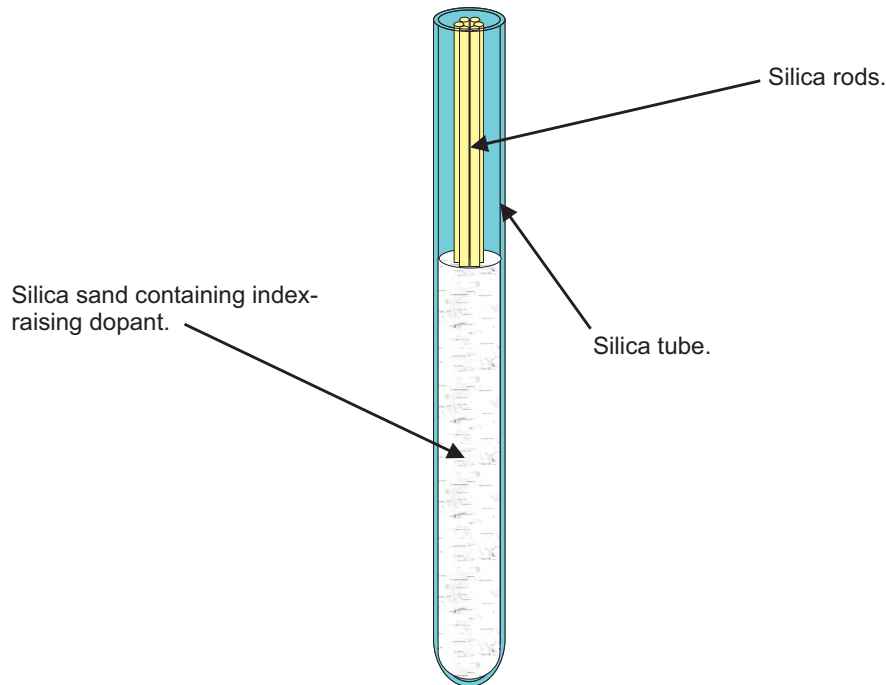


Figure 2. Assembled LCF-preform using the powder-in-tube method.

2. SIMULATIONS

All simulations mentioned here were carried out on the one row hexagonal structure using circular structural elements (figure 1). The search for convenient geometrical parameters which allow for effective single mode operation in this structure has been carried out repeatedly.^{10,11,15,19} The goal of our simulations is to find out, if this geometry is suitable for designs, in which the structure consists of pure silica and the surroundings of aluminum doped silica. It is further assumed, that the index step is such, that it is realisable with the powder-in-tube method.

The one-row hexagonal geometry allows for the variation of two parameters: structural element diameter d and their distance a . The former takes on values between 0 and a : larger values would result in overlapping between the elements. Conversely, for the same reason, the latter takes on values between d and ∞ . It is thus meaningful, to use the parameter d/a for simulation purposes. (The case $a=0$ corresponds to no distance between the elements at all, which is a useless case). As the main focus is on the maximisation of the core diameter, this is the second parameter used in our simulations. For this type of fibre structure, there is no fixed boundary between core and cladding, which leaves some kind of freedom in the choice of what combination of parameters to choose as a measure of the core size. A rather intuitive choice is the radius of the circle tangent to the inner edges of the structure elements ρ which can be expressed as $2\rho=2a-d$.

The low-index structure of silica based leakage channel fibres has mostly been realised either with air holes in silica¹⁰ or fluorine doped rods in silica.¹⁹ The idea of this work is to use pure silica for the structural elements, while the surroundings consist of glass with a refractive index higher than the one of silica. The structure has been implemented in the software package MODE solutions, developed by the Lumerical Company. The waveguide modes are calculated with helps of a finite difference method, solving Maxwell's equations.²³ For two dimensional waveguides, Maxwell's equations take the form of an eigenvalue-equation. Thus, in the context of this finite difference method, the differential equations are transformed into a matrix-eigenvalue equation. Beside the mode profiles, which correspond to the eigenvectors, the propagation constants, which are the corresponding eigenvalues, are calculated. For leaky modes, the latter can take on non-real values.¹³ The imaginary part of this complex numbers thus correspond to the propagation losses of the leaky modes (which are not to be confused with material losses due to scattering and absorption). An important aspect to point out is the proper choice

of boundary conditions. Hard boundary conditions such as perfect electrical conductors do not fully take into account the leaky nature of the waveguide modes, as they physically act as partial transverse reflectors resulting in biased loss calculations. This problem is largely solved by the use of perfectly matched layers (PML) at the boundaries, which mimic the infinite extend of the cladding by absorbing the field energy at the boundary²⁴ (thus an infinite cladding is assumed for calculations). It is further supposed that all parts of the structure are perfectly homogeneous dielectrics with fixed refractive indices which are $n_{str}=1.45$ for the structural elements and $n_{clad}=1.46$ for the cladding. Calculations are executed at fixed wavelength, which in this case is $\lambda=1.064\mu\text{m}$. Initially, one needs to establish a criterion for what shall be considered "effectively single-mode". In this regard, it has been proposed, that a fundamental mode loss of 0.1dB/m and a higher order mode loss of 1dB/m corresponds to a high enough loss difference.¹⁰ In order to determine geometries which fulfill this criterion, mode losses need to be calculated for each pair of parameters (i.e. ρ and d/a). It has been claimed,¹¹ that propagation losses increase with the order of the mode, which is the reason why modes with orders superior to two are not considered here. What is from now on referred to as the "second" or "higher order mode" is the group of modes whose specimens show two intensity maxima in azimuthal direction ("LP₁₁-like"; in analogy to step-index fibre Bessel-modes). Dong, Peng and Li have shown¹¹ that there is little difference between the propagation losses among specimens of this group of modes. It is thus considered sufficient to choose one of these modes. For illustration purposes, the fundamental mode as well as the higher order mode chosen are showed on figures 3 and 4.

The core radius as defined above has been fixed to $\rho=25\mu\text{m}$. In order to determine appropriate geometries, the parameter d/a has been varied and losses of the two lowest order modes have been calculated for each value. The results are illustrated on figure 5 with two vertical lines, delimiting the range for d/a which allows for effective single mode operation according to the aforementioned criterion.

From a practical viewpoint, fundamental mode bend losses are an important parameter. In order to simulate bend behaviour of modes and especially to calculate losses, the mode solver from MODE Solutions can be modified in a way, which transforms Cartesian to toroidal coordinates. It may be noted that the resulting losses correspond to the sum of propagation and bend losses. On figure 6 the bend losses are plotted as a function of bend radius. The bend radius for which the loss is 1dB/m (represented by a horizontal line on figure) corresponds to the so-called "critical" bend radius.¹⁹

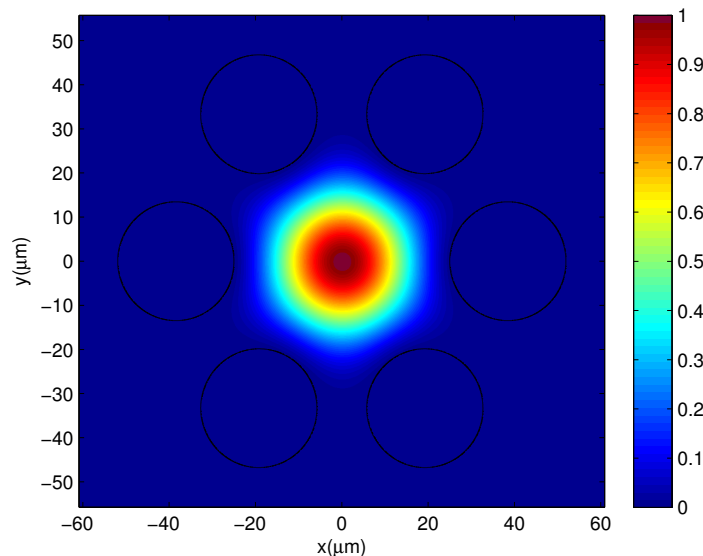


Figure 3. Intensity profile of the fundamental mode of a one-row-hexagonal LCF. The black circles delimit the position of the structural elements. ($\rho=25\mu\text{m}$, $d/a=0.7$, $\Delta n=0.01$).

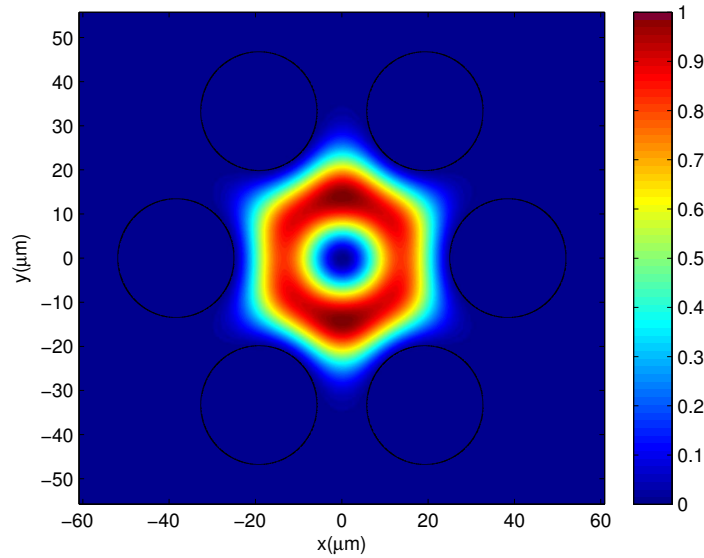


Figure 4. Intensity profile of the second order mode of a one-row-hexagonal LCF. The black circles delimit the position of the structural elements. ($\rho=25\mu\text{m}$, $d/a=0.7$, $\Delta n=0.01$).

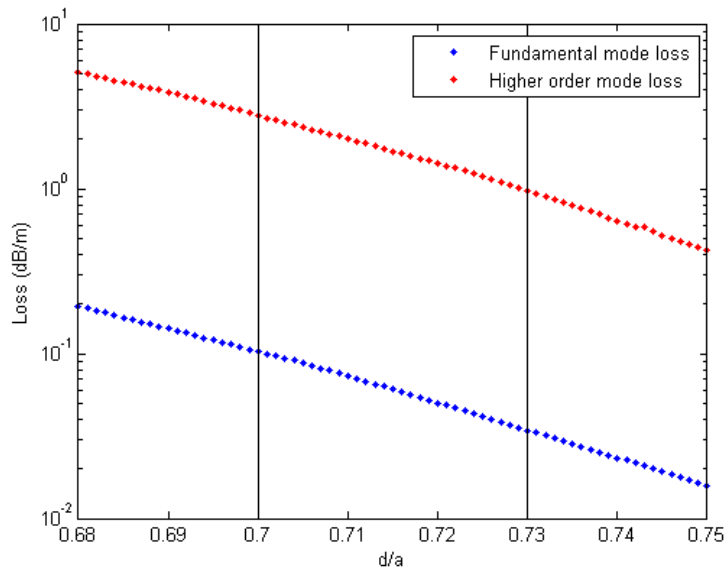


Figure 5. Fundamental and higher order mode propagation losses as a function of d/a with fixed core radius $\rho=25\mu\text{m}$ ($\Delta n=0.01$). The black vertical lines delimit the parameter range, for which the structure is effectively single mode (with the criterion mentioned in the text).

3. EXPERIMENTS

Two fibres have been fabricated implementing the one-row hexagonal design (as on figure 1). As mentioned in the introduction, the structural elements consist of pure silica rods placed inside a closed silica tube. In order to keep the rods transversely in position, we used circular silica plates with the up-scaled structure cut out. The inner diameter of the glass tube is 17mm, the outer diameter 21mm. The silica plates with the transversely inscribed structure have a diameter of 16mm with hole diameter of 1.4mm (corresponding to the silica rods used)

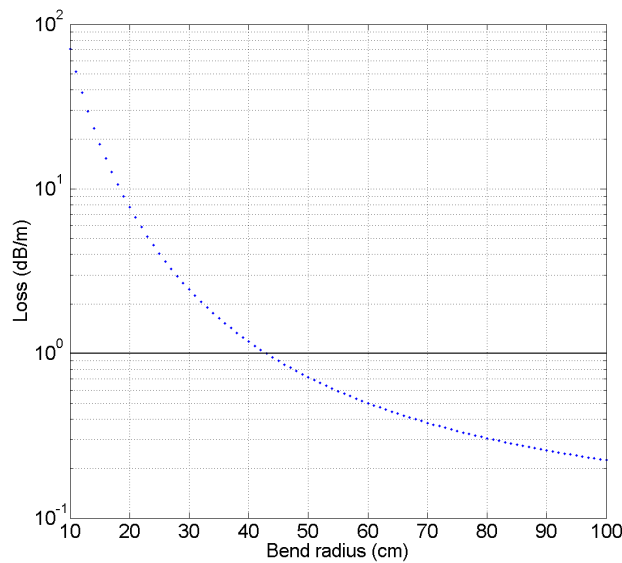


Figure 6. Propagation loss as a function of bend radius for a one-row-hexagonal LCF. ($\rho=25\mu\text{m}$, $d/a=0.7$, $\Delta n=0.01$).

and a hole distance of 2mm. This corresponds to $d/a=0.7$. The aimed fibre diameter is $400\mu\text{m}$ which leads to a core diameter $2\rho=50\mu\text{m}$.

For the fabrication of the Al-doped powder, we had two methods at our disposition: Firstly, the direct mixing of SiO_2 and Al_2O_3 in powder form with its known limitations.²⁵ The second method is based on the sol-gel process. Thus the desired ingredients (in this case Si and Al) are bound in liquid precursors which are heated to $70\text{--}80^\circ\text{C}$ and stirred until gelation sets in. With the helps of a drying process specially developed for this purpose, the undesired contents of the mixture are largely eliminated. The resulting powder then goes through a sintering process, in which it is heated up to 1550°C in steps of $2^\circ\text{C}/\text{min}$, kept at this temperature for three hours and recooled to room temperature. Besides the elimination of remaining impurities, a densification takes place, which allows for the selection of a desired grain size distribution. This method has been applied successfully to the fabrication of Yb-/Al-/P- doped material, in which high homogeneity has been achieved.^{26,27} It has to be noted, that the results concerning the Al-doped powder presented here are preliminary, because no detailed optimisation of grain size the sintering process as well as drawing temperature has yet been carried out. the vitrification of large preforms has not yet been implemented.

The relation between the amount of aluminium oxide and refractive index difference was shown to be linear.²⁸ According to this, a molar concentration of $C_{\text{Al}_2\text{O}_3}=4\%\text{mol}$ in the glass batch corresponds to a refractive index difference of $\Delta n=10^{-2}$. On this basis, a sol-gel based granulate has been fabricated. The densified block coming out of the sintering process was crushed to small pieces by a manually operated pestle and particle sizes between $150\mu\text{m}$ and 1mm sieved out. For the preform of this fibre, position holders with a thickness of 5mm were fabricated with the helps of a waterjet cutting machine. The assembled preform was drawn to a fibre. As it can be seen on figure 7, the surroundings show that a homogeneous glass was formed during fibre drawing. This is confirmed by the refractive index profile (figure 8) which enables the measurement of the achieved index difference which is about $\Delta n=(4.3 \pm 0.3) \cdot 10^{-3}$. The fibre diameter, however, is only $179\mu\text{m}$, which is due to drawing conditions. Along with the small index step, this leads to a fundamental mode loss of about $15\text{dB}/\text{m}$, what along with still not fully eliminated scattering losses makes it impossible to measure an intensity profile. Loss measurements on sol-gel fabricated Yb-/Al-/P-doped powder, however, indicate that the latter can be mitigated.

For the cladding material of the second fibre, the components were directly mixed in oxide form. This leads to a somewhat grainy structure, as it can be seen on figure 9 (along with a high-contrast image of the first fibre for comparison). This leads to the conclusion, that the sol-gel method leads to much improved homogeneity

and that an LCF with silica structural elements with performance (in terms of mode field area) comparable to reported models with fluorine doped elements¹⁴ is very close to implementation.

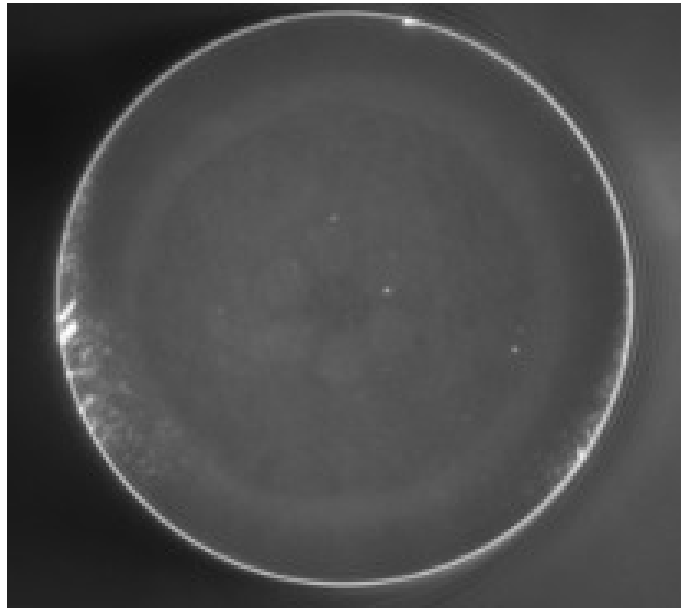


Figure 7. Microscope image of the LCF with sol-gel based cladding material. The outer diameter is $179\mu\text{m}$.

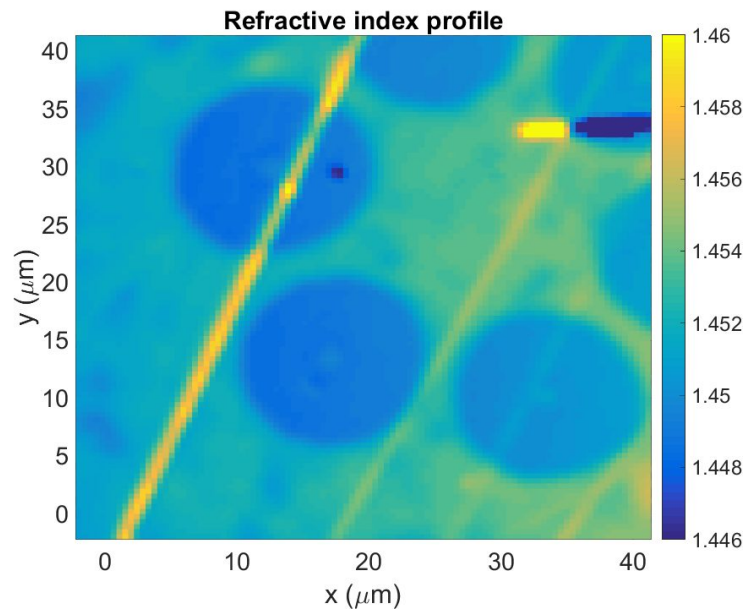


Figure 8. Refractive index profile of the LCF with sol-gel based cladding material. The striae are due to sample preparation for the refractive index profiling.

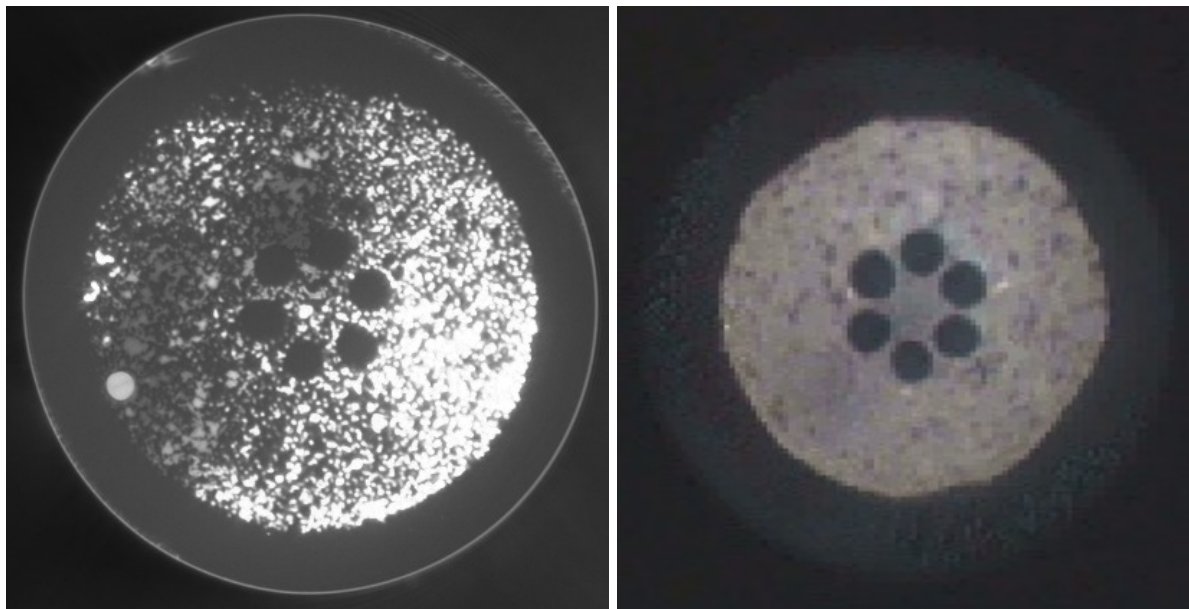


Figure 9. Microscope images of both LCFs drawn. Left: Material fabricated by direct oxide mixing (outer diameter is $317.9\mu\text{m}$). Right: Material fabricated by sol-gel process ($179\mu\text{m}$).

4. CONCLUSION AND OUTLOOK

In sum, the feasibility of an all-glass leakage channel fibre using the powder-in-tube method with a high-index cladding using sol-gel fabricated granulate and pure silica structure elements has been demonstrated. The simulations show that the parameter range, in which effective single mode operation is possible, leads to a high enough geometrical degree of freedom which allows for the realisation of the concept. Although the guiding properties have not yet been verified experimentally, the experiments prove that the aimed structure element arrangement is realisable.

Furthermore, the sol-gel based fabrication and grain size selection of the powder has proved to have positive influence on homogeneity and the refractive index step is close to the intended value.

The main challenges in the practical realisation of the proposed fibre design lie in the further optimisation of composition and texture of the powder material. This will be tackled by trying out different particle size distributions and different dopants (e.g. germanium or titanium).

Once we have drawn an LCF which has a glass quality which makes it capable of guiding light with acceptable losses, we will carry out loss measurements. Apart from overall losses, we plan to measure the actual mode distribution, which will determine whether the fibre is operating in the effective single mode regime or not.

REFERENCES

- [1] Zervas, M. and Codemard, C., "High power fiber lasers: A review," *IEEE J. Sel. Top. Quantum Electron.* **20**, 0904123 (2014).
- [2] Offerhaus, H., Broderick, N., Richardson, D., Sammut, R., Caplen, J., and Dong, L., "High-energy single-transverse-mode q-switched fiber laser based on a multimode large-mode-area erbium-doped fiber," *Opt. Lett.* **23**, 1683–1685 (1998).
- [3] Koplow, J., Kliner, D., and Goldberg, L., "Single-mode operation of a coiled multimode fiber amplifier," *Opt. Lett.* **25**, 442–444 (2000).
- [4] Fermann, M., "Single-mode excitation of multimode fibers with ultrashort pulses," *Opt. Lett.* **23**, 52–54 (1998).

- [5] Knight, J., Birks, T., Cregan, R., Russell, P., and de J.P. Sandro, "Large mode area photonic crystal fibre," *Electron. Lett.* **34**, 1347–1348 (1998).
- [6] Limpert, J., Liem, A., Reich, M., Schreiber, T., Nolte, S., Zellmer, H., Tnnermann, A., Broeng, J., Petersson, A., and Jakobsen, C., "Low-nonlinearity single-transverse-mode ytterbium-doped photonic crystal fiber amplifier," *Opt. Express* **12**, 1313–1319 (2004).
- [7] Knight, J., Birks, T., Russell, P. S., and de Sandro, J., "Properties of photonic crystal fiber and the effective index model," *J. Opt. Soc. Am. A* **15**, 748–752 (1998).
- [8] Monro, T., Bennett, P., Broderick, N., and Richardson, D., "Holey fibers with random cladding distributions," *Opt. Lett.* **25**, 206–208 (2000).
- [9] Limpert, J., Deguil-Robin, N., Manek-Hnninger, I., Salin, F., Rser, F., Liem, A., Schreiber, T., Nolte, S., Zellmer, H., Tnnermann, A., Broeng, J., Petersson, A., and Jakobsen, C., "High-power rod-type photonic crystal fiber laser," *Opt. Express* **14**, 1055–1058 (2005).
- [10] Wong, W., Peng, X., McLaughlin, J., and Dong, L., "Breaking the limit of maximum effective area for robust single-mode propagation in optical fibers," *Opt. Lett.* **30**, 2855–2857 (2005).
- [11] Dong, L., Peng, X., and Li, J., "Leakage channel optical fibers with large effective area," *J. Opt. Soc. Am. B: Opt. Phys.* **24**, 1689–1697 (2007).
- [12] Saitoh, K., Tsuchida, Y., Rosa, L., Koshiba, M., Poli, F., Cucinotta, A., Selleri, S., Pal, M., Paul, M., Ghosh, D., and Bhadra, S., "Design of effectively single-mode leakage channel fibers with large mode area and low bending loss," *Opt. Express* **17**, 4913–4919 (2009).
- [13] Hu, J. and Menyuk, C., "Understanding leaky modes: slab waveguide revisited," *Adv. Opt. Photonics* **1**, 58–106 (2009).
- [14] Dong, L., McKay, H., Fu, L., Ohta, M., Marcinkevicius, A., Suzuki, S., and Fermann, M., "Ytterbium-doped all glass leakage channel fibers with highly fluorine-doped silica pump cladding," *Opt. Express* **17**, 8962–8969 (2009).
- [15] Tsuchida, Y., Saitoh, K., and Koshiba, M., "Design of single-moded holey fibers with large-mode-area and low bending losses: The significance of the ring-core region," *Opt. Express* **15**, 1794–1803 (2007).
- [16] Hu, D., Luan, F., and Shum, P., "All-glass leakage channel fibers with triangular core for achieving large mode area and low bending loss," *Opt. Commun.* **284**, 1811–1814 (2011).
- [17] Rastogi, V. and Chiang, K., "Holey optical fiber with circularly distributed holes analyzed by the radial effective-index method," *Opt. Lett.* **28**, 2449–2451 (2003).
- [18] Poli, F. and Selleri, S., "Single air-hole ring polygonal photonic crystal fibers with reduced bending loss and field distortion," in [*Transparent Optical Networks, 2008. ICTON 2008. 10th Anniversary International Conference on*], Marciniak, M., ed., *Proc. IEEE* **2**, 60–63 (2008).
- [19] Dong, L., Wu, T., McKay, H., Fu, L., Li, J., and Winful, H., "All-glass large-core leakage channel fibers," *IEEE J. Sel. Top. Quantum Electron.* **15**, 47–53 (2009).
- [20] Pal, M., Paul, M., Mahanty, T., Ghosh, D., Bhadra, S., Rosa, L., and Saitoh, K., "Design and fabrication of f-doped large mode area leakage channel fiber," in [*OptoElectronics and Communications Conference (OECC), 2010 15th*], IEEE, ed., *Proc. IEEE* **1**, 784–785 (2010).
- [21] Knight, J., Birks, T., Russell, P., and Atkin, D., "All-silica single-mode optical fiber with photonic crystal cladding," *Opt. Lett.* **21**, 1547–1549 (1998).
- [22] Ballato, J. and Snitzer, E., "Fabrication of fibers with high rare-earth concentrations for faraday isolator applications," *Appl. Opt.* **34**, 6848–6854 (1995).
- [23] Zhu, Z. and Brown, T., "Full-vectorial finite-difference analysis of microstructured optical fibers," *Opt. Express* **10**, 853–864 (2002).
- [24] Rogier, H. and Zutter, H. D., "Berenger and leaky modes in optical fibers terminated with a perfectly matched layer," *J. Lightwave Technol.* **20**, 1141–1148 (2002).
- [25] Romano, V., Etissa, D., and Pilz, S., "Sol-gel based doped granulated silica for the rapid production of optical fibers," *Int. J. Mod Phys B* **28**, 1442010–1–1442010–20 (2014).
- [26] Najafi, H., "Atomic-scale imaging of dopant atoms and clusters in yb-doped optical fibers," in [*SPIE Photonics Europe 2016*], SPIE, ed., *Proc. SPIE* **9886**, paper 35 (2016).

- [27] Pilz, S., “Progress in the fabrication of optical fibers by the sol-gel-based granulated silica method,” in [*SPIE Photonics Europe 2016*], SPIE, ed., *Proc. SPIE* **9886**, paper 40 (2016).
- [28] Bubnov, M., Vechkanov, V., Guryanov, A., Zotov, K., Lipatov, D., Likhachev, M., and Yashkov, M., “Fabrication and optical properties of fibers with an Al_2O_3 - P_2O_5 - SiO_2 glass core,” *Inorg. Mater.* **45**, 444–449 (2009).